

## A SIMULINK MODEL OF THE 4-PHASE SWITCHED RELUCTANCE MOTOR DRIVE

V. Trifa, Ramona Galatus  
 Department of Electrical Drives and Robots  
 Technical University of Cluj  
 15 C. Daicoviciu St.  
 RO-3400 Cluj-Napoca, Romania

*Abstract- Mathematical modeling and simulation of the 4-phase 8/6 switched reluctance motor (SRM) drive is presented, using Matlab 5.2 with Simulink 2.0 environment. The architecture of the model consists of an 8/6 SRM with 4 opto-electronic sensor angular transducer, a unipolar PWM inverter and a logic control unit. The large number of parameters and variables recommends Simulink model as being the most appropriate for the investigation of SRM drive by numerical simulation. There are considered voltage equations of the motor and a PWM of current source-type inverter. Logic control unit module allows the switching the inverter control among the five modes of operation: normal, boost, long-dwell, two-phase-on and brake. There are shown various simulation results in respect to electrical and mechanical magnitudes and there is also given a comparison with experimental results.*

### I. INTRODUCTION

The SRM models have as main objective to analyze the commutation of its phases in order to improve static and dynamic characteristics. Recent studies on SRM commutation are usually devoted to two problems: 1. The optimum switching angles and how they may be calculated or found experimentally, respectively 2. The strategy of control for sensors installed in definite position to ensure the best or optimal power and

dynamic SRM characteristics. The paper deals with the second problem, concerning the commutation process of an 8/6 SRM.

Simulink model of the SRM drive has been built as it contains logic modules that allow investigating various control modes with 4-quadrant operation. The model starts from SRM stator-rotor configuration, as depicted in figure 1.

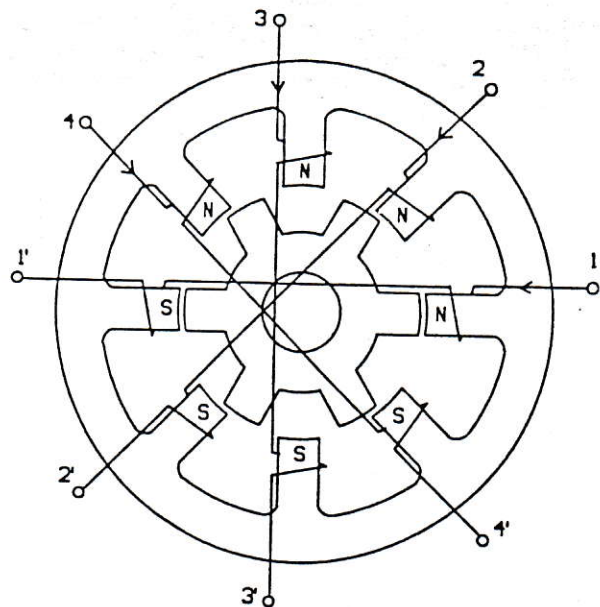


Figure 1. Stator-rotor laminations of 4-phase SRM.

Each phase consists of two diametrically opposite windings that produce north poles on half of stator poles and south poles on the second half. This magnetic orientation determines mutual inductivities practically

null and consequently an important simplification of mathematical model of SRM is obtained.

SRM phases can be controlled in two ways: 1. Time control, which is similar to open-loop stepping motors [1], but is not convenient for SRM due to rotor oscillations and 2. Space control, which refers to self-commutation of motor phases with respect to rotor position, which is preferable for SRM. The space control involves rotor-angle detection and adequate logic control. As result SRM can reach thousands of rpm with acceptable ripples of electromagnetic torque.

### II. COMMUTATION OF SRM PHASES

A 4-quadrant operation of SRM is possible when a multi-sensor angular transducer is chosen. For the particular chace of 4-phase 8/6 SRM there are used 4 sensors A-B-C-D, placed on the stator as shown in figure 2.

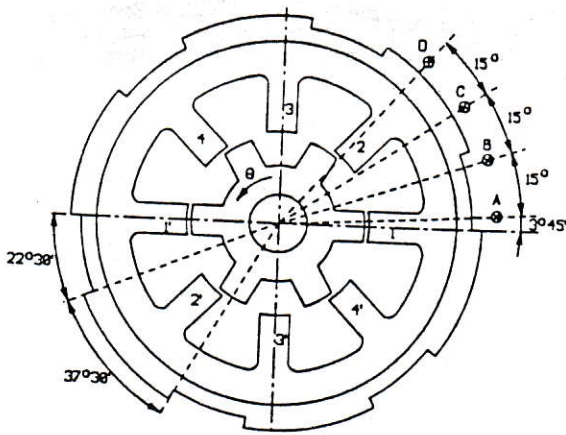


Figure 2. 8/6 SRM geometry with position sensors

The sensors are of opto-electronic type and they are excited by a slotted disk mounted on rotor shaft, as it is represented on external circumference of figure 2. Sensor A axis is shifted with  $3.75^\circ$  with respect to phase 1 axis, as calculated with expression [2]:

$$\theta_{sh} = \frac{180^\circ}{2Sz_r} = 3.75^\circ \quad (1)$$

where  $S$  is the number of sensors ( $S=4$ ) and  $z_r$  is the number of rotor poles ( $z_r=6$ ). Transducer disk contains 6 slots of  $30^\circ - 2\theta_{sh}=22.5^\circ$ . This geometry gives the symmetry of operation in the forward-reverse directions of SRM.

By logical processing of the 4-transducer signals A-B-C-D, the control pulses f1-f4 for SRM phases are deduced. Several modes of logical combinations are available, which give distinct operation modes of the motor. They are depicted in figure 3, taking as reference the variation of phase 1 inductivity.

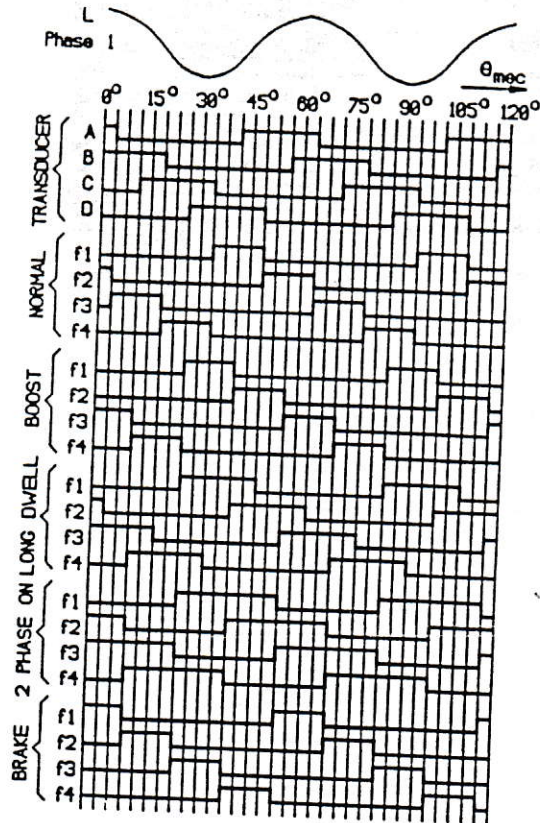


Figure 3. Angular transducer and phase control signals

- a) normal mode - which corresponds to one-phase-on supplying of motor phases 1-2-3-4, with a

- commutation angle of  $\theta_{sh}=3.75^\circ$  behind the unaligned rotor position (with respect to phase 1);
- b) boost mode – also one-phase-on supplying with a commutation angle of  $\theta_{sh}$  before unaligned rotor position;
- c) long-dwell mode – with the same commutation angle as boost mode, but each phase is maintained energized for an extra  $2\theta_{sh}$  angle. In this case a superposition of  $2\theta_{sh}$  of phase supplying is obtained;
- d) two-phase-on mode – with the same commutation angle as boost and long-dwell modes, but with an extra supply of  $2\theta_{sh}$  with respect to long-dwell mode. In this case a classical two-phase-on supply is produced;
- e) brake mode – in which motor phases are supplied in one-phase-on sequence with a commutation angle of  $\theta_{sh}$  before the aligned rotor position, that is on negative slope of inductivity.

The five modes of operation are distinct by proper logic combinations of transducer signals A-B-C-D, as given in table I, for forward operation (trigonometric direction).

Table I

phase	normal	boost	long-dwell	2-phase-on	brake
f1	$\overline{BCD}$	$\overline{ABD}$	D	D+ $\overline{AB}$	$\overline{BCD}$
f2	$\overline{ACD}$	$\overline{ABC}$	A	A+ $\overline{CD}$	$\overline{ACD}$
f3	$\overline{ABD}$	$\overline{BCD}$	B	B+ $\overline{CD}$	$\overline{ABD}$
f4	$\overline{ABC}$	$\overline{ACD}$	C	C+ $\overline{AB}$	$\overline{ABC}$

Combinatorial logic for providing phase control signals  $f_1$ – $f_4$  can be implemented by PROM-memories or PLA-circuits, or by a microprogrammed system with a special purpose controller or a microprocessor [3]. For reverse direction a mirror copy of the signals from figure

3 is considered, provided the transducer shift angle is  $\theta_{sh}=3.75^\circ$ .

### III. THE SIMULINK MODEL

The drive model originates from SRM equations, which are written with the following assumptions:

- mutual inductivities are null, as shown before;
- leakage inductivities are neglected;
- self-inductivities are of sinusoidal shapes with respect to rotor angle, as deduced from experimental measurements [4];
- magnetic saturation is neglected for an easier investigation.

The voltage equation of phase k is:

$$u_k = R_k i_k + \frac{dL_{kk}}{d\theta} \frac{d\theta}{dt} i_k + L_{kk} \frac{di_k}{dt} \quad (2)$$

where  $L_{kk}$  is self-inductivity of phase k and  $\theta$  is electrical angle, deduced from mechanical angle with:

$$\theta = z, \theta_{mec} \quad (3)$$

A simplified sinusoidal variation of phase inductivity is considered:

$$L_{kk} = L_0 + L_1 \cos\left(\theta - \frac{k-1}{2}\pi\right), \quad (4)$$

where  $L_0$  and  $L_1$  are average, respectively amplitude of inductivity variation, which are calculated from:

$$L_0 = \frac{L_d + L_q}{2}, \quad L_1 = \frac{L_d - L_q}{2} \quad (5)$$

$L_d$  represents the phase inductivity for aligned rotor position and  $L_q$  for unaligned position.

Mathematical model of SRM is given by state equations deduced from expression (2), where new notations appear as follows:

$$\frac{di_k}{dt} = \frac{1}{L_0 + L_1 \cos(\theta - \frac{k-1}{2}\pi)} [u_k - Ri_k + \omega L_1 i_k \sin(\theta - \frac{k-1}{2}\pi)], \quad k = 1 \div 4$$

$$\frac{d\omega}{dt} = -\frac{z_r^2 L_1}{2J} \sum_{k=1}^4 i_k^2 \sin(\theta - \frac{k-1}{2}\pi) - \frac{B}{J} \omega - \frac{z_r M_r}{J} \text{sign}(\omega) \quad (6)$$

$$\frac{d\theta}{dt} = \omega$$

$R$  - phase resistance

$\square$  - angular speed [electrical radians/sec]

$J$  - total rotor moment of inertia

$B$  - coefficient of viscous friction

$M_r$  - load torque, of reactive type.

The four voltages  $u_1+u_4$  correspond to unipolar PWM supplying provided by a current source-type inverter. A hysteresis unit that processes the voltage between  $-60V$  and  $+60V$  with an average current up to  $9A$ , models the PWM inverter.

The whole model of SRM drive is depicted in figure 4. This model allows 4-quadrant operation of SRM with symmetrical behavior referring to forward and reverse direction. Four modes for forward direction (normal, long-dwell, two-phase-on and brake) are implemented through manual switches. In this way it is possible on-line switching among the 4 modes and the control of forward-reverse directions. As result 4-quadrant operation of SRM can be investigated.

As control mode is periodical after  $16 \times 3.75^\circ$  (see

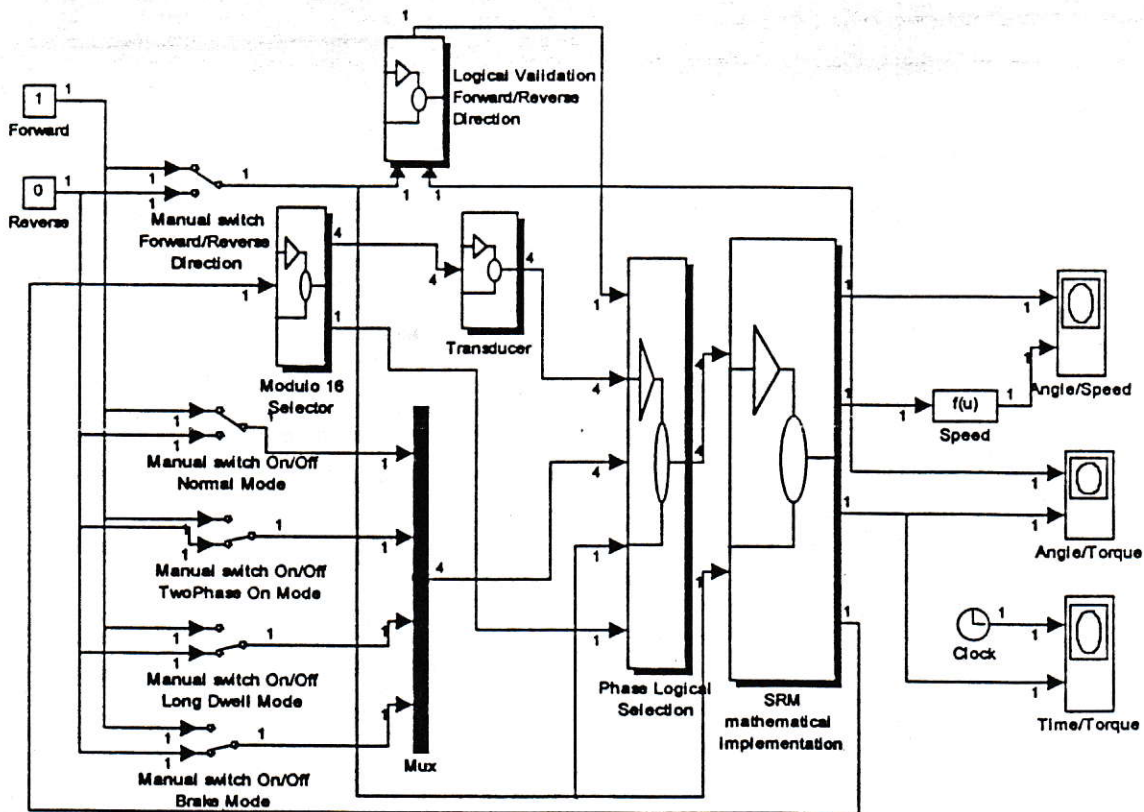


Figure 4. Simulink model of SRM

figure 3), a modulo 16 counter is considered in order to select the transducer signals. These signals are stored in a 16-row/4-column matrix. Mode and direction of operation are logical implemented through a Phase Logical Selection unit. Direction enabling logic generates signals for changing the operation sense.

**IV. SIMULATION RESULTS**

Numerical specifications of SRM drive are given below:

$R = 0.24 \Omega$ ,  $L_0 = 0.007 \text{ H}$ ,  $L_1 = 0.003 \text{ H}$ ,  $M_r = 0.1 \text{ Nm}$ ,  
 $J = 26 \times 10^{-6} \text{ Nms}^2$ ,  $B = 0.001 \text{ Nms}$ ,  $I = 9 \text{ A}$  (phase current amplitude),  $\Delta I = 0.9 \text{ A}$  (current PWM ripples),  $V = 60 \text{ V}$  (supply voltage).

A lot of simulation results can be obtained from Simulink model. Among these results, several representative curves are selected.

Figure 5 and 6 show phase voltages and currents variations during motor acceleration under constant load.

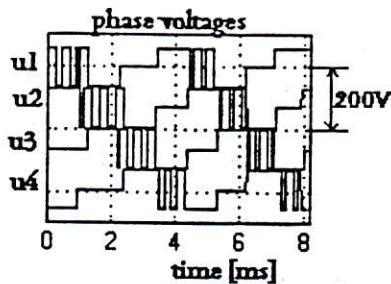


Figure 5. Phase voltages

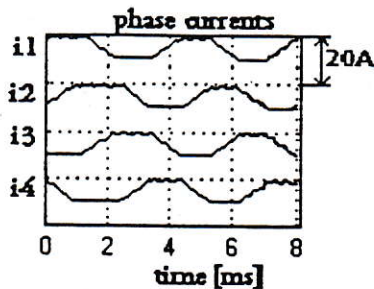


Figure 6. Phase currents

Unipolar trapezoidal shapes of the currents, as result of PWM voltages are observed.

Four-quadrant operation of the SRM is shown in figures 7 and 8, with respect to speed versus angle variation and electromagnetic torque versus time variation.

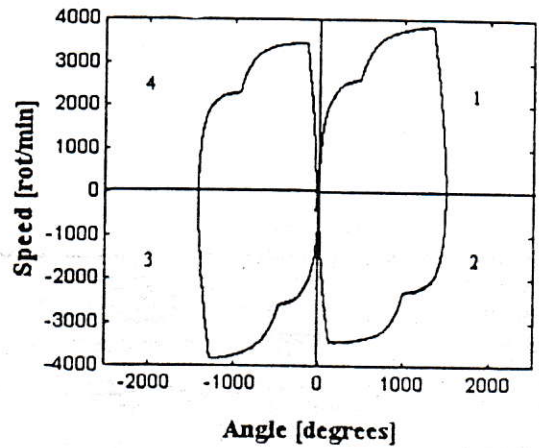


Figure 7. Speed cycles

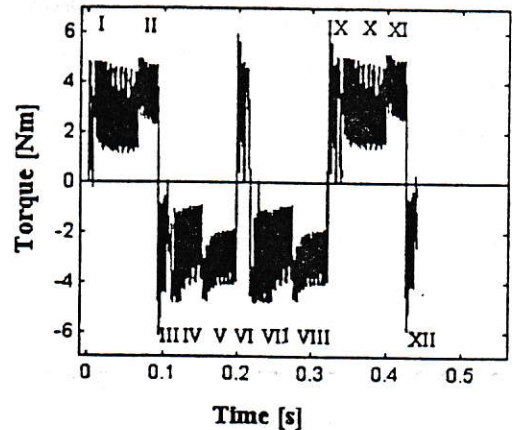


Figure 8. Torque variation

Speed cycles are obtained from a sequence of modes as illustrated in figure 7: forward with normal, long-dwell and brake modes (1 and 4), backward with symmetrical modes (2 and 3). Torque variation that produces the illustrated speed cycle is given in figure 8 and comprises 12 steps such as:

I+II+III – speed cycle of quadrant 1 (figure 7)

IV+V+VI – speed cycle of quadrant 2

VII+VIII+IX – speed cycle of quadrant 3

X+XI+XII – speed cycle of quadrant 4

Figures 9 and 10 show the variation of speed and torque at a small time scale.

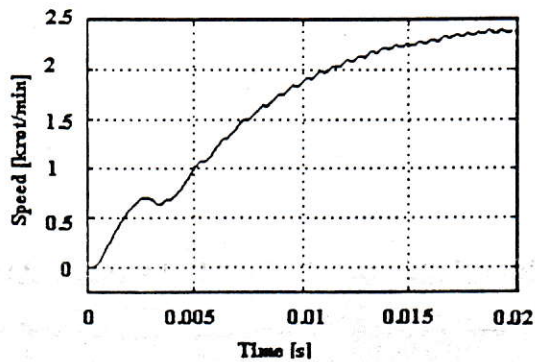


Figure 9. Speed variation in normal mode

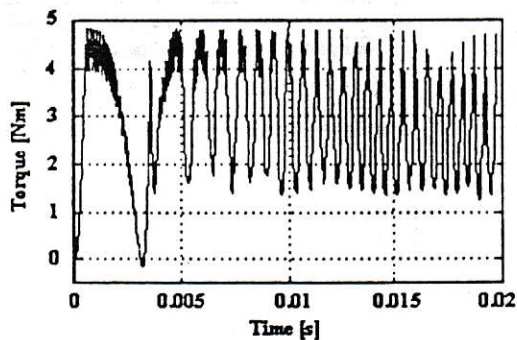


Figure 10. Torque variation in normal mode

As expected, at motor start the speed is influenced by the torque variation. This variation is caused by current oscillations, which are determined by both PWM ripples and trapezoidal or triangular shapes produced by sequential feeding of motor phases.

A slightly better behavior is observed in long-dwell mode, when torque ripples are smaller than in normal mode. Figure 11 shows the torque variation at motor start in long-dwell mode.

The torque ripples are now in attention of practitioners, who make efforts to find methods for minimization the vibrations and noise of SRM [5].

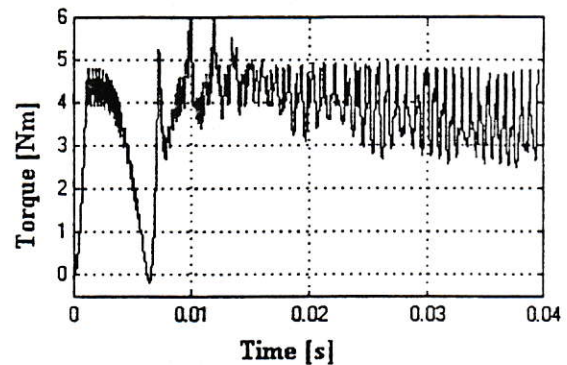


Figure 11. Torque variation in long-dwell mode

Mechanical speed versus torque characteristics can be also deduced from Simulink model. First, SRM starting under various load torques between 0.1 and 0.4 Nm, for normal operation, is shown in figure 12. The simulation goes on until the speed is stabilized at a constant value dependant of load torque magnitude. The motor start has been also considered for long-dwell mode. As result speed/torque static characteristics are obtained, as illustrated in figure 13.

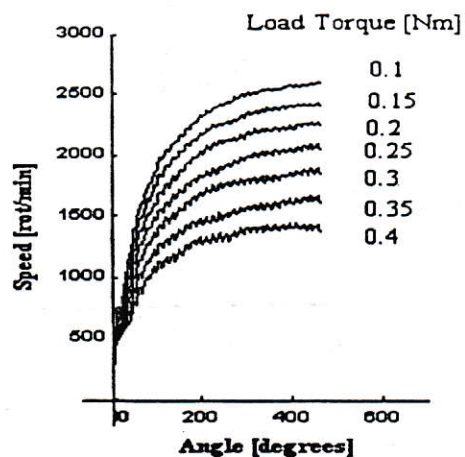


Figure 12. SRM starting in normal mode

Experimental set-up arrangement consisting of 4-phase 8/6 SRM driven by a PWM inverter of current source has been considered. The control part has been built with PC-based acquisition card LabVIEW L1200, made by National Instruments [6]. Real characteristics

have been obtained and a satisfactory superposition on simulated characteristics.

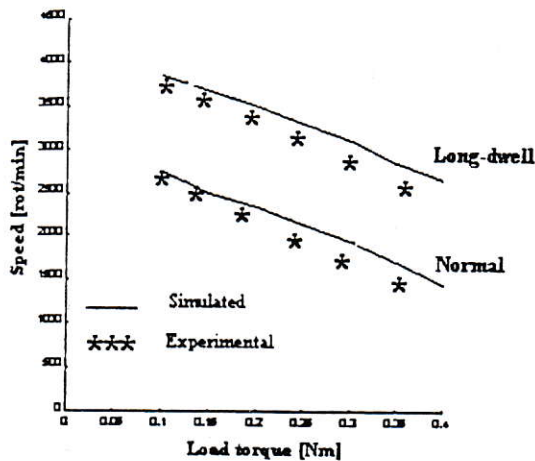


Figure 13. Speed-torque characteristics

Some differences appear for high load torque, when the influence of magnetic saturation is significant.

## V. CONCLUSIONS

Simulink model of SRM has been found most appropriate to study the commutation aspects, as they involve logic signals and combinatorial processing. A simplified mathematical model has been used with satisfactory results. A large palette of simulation procedures is available through simple manual switches. 4-quadrant operation of SRM has been investigated taking into account the variation of mechanical magnitudes such as speed and electromagnetic torque. Finally, static mechanical speed versus torque characteristics are deduced and compared to experimental ones. It is obtained a good superposition of results.

## VI. REFERENCES

- [1] Kuo, B.C., Kelemen, A., Crivii, M., Trifa, V. "Incremental Motion Control and Regulation Systems" (in Romanian), Ed. Tehnica, Bucharest, 1981, 532 pag.
- [2] Becerra, R.C., Ehsani, M., Miller, T.J.E., "Commutation of SR Motors", *IEEE Transactions of Power Electronics*, Volume 8, No.3, July 1993, pages 257-263.
- [3] Miller, T.J.E., "Switched Reluctance Motors and Their Control", Magna Physics Publishing and Clarendon Press, Oxford, 1993, 205 pag.
- [4] Trifa, V., Marschalko, R., Ramona Gălătuș, Szekely, A., "Investigations concerning the modelling of switched reluctance motor drives", *Proceedings of A&Q International Conference on Automation and Quality Control*, Technical University of Cluj, Romania, June 1998, pages A402-407.
- [5] O'Donovan, J.G., Roche, P.J., Kavanagh, R.C., Egan, M.G., Murphy, J.M.D. "Neural Network Based Torque Ripple Minimisation in a Switched Reluctance Motor". *IEEE Transaction on Industrial Applications*, 1994, pages 1226-1231.
- [6] Trifa, V., Marschalko, R., Szekely, A., Szasz, Cs., Ramona Gălătuș, "Investigation of a four phase switched reluctance motor supplied from a PWM inverter". *Proceedings of 6th OPTIM'96 Conference*, Brasov, Romania, Volume 2, May 1998, pages 341-344.